

# UC Irvine

## UC Irvine Previously Published Works

### Title

O17 NMR study of local spin susceptibility in aligned YBa<sub>2</sub>Cu<sub>3</sub>O<sub>7</sub> powder

### Permalink

<https://escholarship.org/uc/item/587013w0>

### Journal

Physical Review Letters, 63(17)

### ISSN

0031-9007

### Authors

Takigawa, M  
Hammel, PC  
Heffner, RH  
[et al.](#)

### Publication Date

1989-10-23

### DOI

10.1103/physrevlett.63.1865

### Copyright Information

This work is made available under the terms of a Creative Commons Attribution License, available at <https://creativecommons.org/licenses/by/4.0/>

Peer reviewed

## $^{17}\text{O}$ NMR Study of Local Spin Susceptibility in Aligned $\text{YBa}_2\text{Cu}_3\text{O}_7$ Powder

M. Takigawa, P. C. Hammel, R. H. Heffner, Z. Fisk, K. C. Ott, and J. D. Thompson

*Los Alamos National Laboratory, Los Alamos, New Mexico 87545*

(Received 23 March 1989)

$^{17}\text{O}$  nuclear-magnetic-resonance spectra are obtained, using uniaxially aligned powder of  $\text{YBa}_2\text{Cu}_3\text{O}_7$ , and resonance lines from the four inequivalent oxygen sites are clearly distinguished. Principal components of the electric-field-gradient (EFG) and the shift tensors are obtained in the normal state. Assigning the direction of the largest EFG components to Cu-O bond axes, the anisotropy of the shift suggests that the spin density at the plane O(2,3) and the bridging O(4) sites resides on the  $p_\sigma$  orbitals. The dominant contribution to the spin susceptibility comes from Cu  $d$  states.

PACS numbers: 74.70.Vy, 74.30.Gn, 76.60.Cq

High-temperature Cu-oxide superconductors are typically in an antiferromagnetic-insulating state when there is one hole in the Cu  $3d$  shell (in the  $\text{CuO}_2$  layer) and are superconducting as the hole concentration exceeds a critical value. There is strong spectroscopic evidence that these additional holes primarily fill orbitals of O  $2p$  character.<sup>1-4</sup> It is therefore important to identify which O site and which orbital ( $p_\sigma$  or  $p_\pi$ ) the holes go into. In particular, the identification of specific hole orbitals in the  $\text{CuO}_2$  planes puts important constraints on theoretical models.<sup>5</sup> We have performed  $^{17}\text{O}$  nuclear-magnetic-resonance (NMR) experiments in oriented powder samples of  $\text{YBa}_2\text{Cu}_3\text{O}_7$  and have identified the NMR lines corresponding to all four inequivalent oxygen sites. The principal values of the electric-field-gradient (EFG) and shift ( $K$ ) tensors show that the spin density at the planar and bridging oxygen sites resides mainly on the  $p_\sigma$  orbitals, indicating that doped holes go into these  $p_\sigma$  orbitals.

A sintered pellet of  $\text{YBa}_2\text{Cu}_3\text{O}_7$  made by standard techniques was enriched with  $^{17}\text{O}$  by heating the sample at  $900^\circ\text{C}$  for 2 h, followed by an anneal at  $470^\circ\text{C}$  for 20 h in an  $\text{O}_2$  (45%  $^{17}\text{O}$ ) atmosphere. This material was then ground into powder and mixed with epoxy (Stycast 1266) in a magnetic field of 4.2 T to achieve a uniaxial alignment of the  $c$  axis for each grain. Good alignment is obtained by this technique as was demonstrated in the Cu NMR spectra published previously.<sup>6</sup> Magnetization measurements confirmed the superconducting transition temperature of 93 K and nearly full shielding. The NMR spectra were obtained by integrating the spin-echo signal with a boxcar integrator while sweeping the applied magnetic field.

There are four inequivalent oxygen sites in a unit cell of  $\text{YBa}_2\text{Cu}_3\text{O}_7$ : one in the copper-oxide chains O(1), four in the two-dimensional ( $\text{CuO}_2$ ) layers O(2) and O(3), and two in the bridging sites between the chains and planes O(4). Since  $^{17}\text{O}$  nuclei have spin  $\frac{5}{2}$ , we expect five resonance lines split by the nuclear quadrupole interaction for each site.

Figure 1 shows the  $^{17}\text{O}$  NMR spectra at 160 K and 49.8 MHz, with the magnetic field applied parallel to the

$c$  axis. Three distinct central transitions (lines  $A_0$ ,  $B_0$ , and  $C_0$ ), corresponding to  $I_z = \frac{1}{2} \leftrightarrow -\frac{1}{2}$ , and four sets of satellite transitions (lines  $B_1$ - $B_4$ ,  $B'_1$ - $B'_4$ ,  $A_1$ ,  $A_2$ , and  $C_1$ ,  $C_2$ ) are observed. Second satellite transitions ( $I_z = \pm \frac{3}{2} \leftrightarrow \pm \frac{5}{2}$ ), whose first satellites ( $I_z = \pm \frac{1}{2} \leftrightarrow \pm \frac{3}{2}$ ) are  $A_1$ ,  $A_2$ , and  $C_1$ ,  $C_2$ , have also been observed, although they are not shown in the figure. From the crystal structure, we know that the crystalline  $\hat{a}$ ,  $\hat{b}$ , and  $\hat{c}$  axes are the principal axes of both the EFG and  $K$  tensors. We define the shift in the resonance frequency as  $\delta\nu = \nu_{\text{res}} - \nu_0$ , where  $\nu_{\text{res}}$  is the NMR frequency and  $\nu_0 = \gamma_N H_{\text{res}}$ .  $H_{\text{res}}$  is external field at the peak of resonance and  $\gamma_N$  is the  $^{17}\text{O}$  gyromagnetic ratio (0.577 186 kHz/Oe, obtained from the resonance in  $\text{H}_2\text{O}$ ). When the direction of the magnetic field ( $z$ ) is along one of the principal axes, we have<sup>7</sup>

$$\delta\nu = \begin{cases} K_z \nu_0 + \frac{2}{9} (\nu_x - \nu_y)^2 / \nu_0, & (1a) \\ K_z \nu_0 \pm \nu_z + \frac{5}{36} (\nu_x - \nu_y)^2 / \nu_0, & (1b) \\ K_z \nu_0 \pm 2\nu_z - \frac{1}{9} (\nu_x - \nu_y)^2 / \nu_0, & (1c) \end{cases}$$

for the central, first, and second satellite lines, respec-

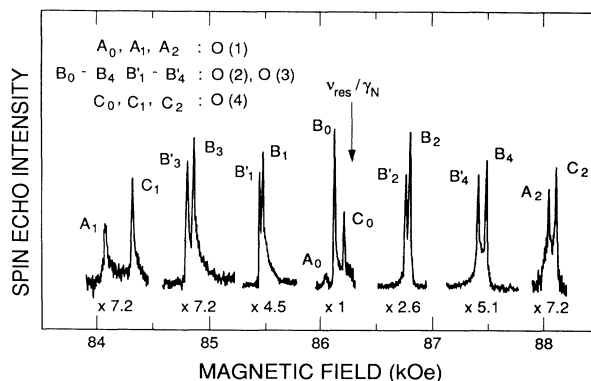


FIG. 1.  $^{17}\text{O}$  NMR spectra at 160 K and 49.8 MHz with magnetic field along the  $c$  axis. Each piece of the spectrum was taken with different gain as shown under the spectra.

tively. Here  $K_z$  is the  $z$  component of the shift,  $v_a = -\frac{3}{20} |eQ| \partial^2 V / \partial a^2$ , where  $Q$  is the nuclear quadrupole moment, and  $\partial^2 V / \partial a^2$  is the  $a$  component of the EFG.

The values of  $K_c$  and  $|v_a - v_b|$  for the three central lines were determined from Eq. (1a) by measuring  $\delta\nu$  at different values of  $\nu_{\text{res}}$  (49.8, 40.2, and 30.2 MHz). (This procedure was also used to determine the Cu Knight shift.<sup>6</sup>) The values of  $\nu_c$  ( $\equiv \nu_z$ ) were determined for each set of satellite lines from the difference between  $\delta\nu$  for the high- and low-field satellite lines. The association of the central line with its satellite lines was accomplished by demanding self-consistency in Eqs. (1a)-(1c). It was found that the two sets of satellites  $B_1-B_4$  and  $B'_1-B'_4$  correspond to the central line  $B_0$ , and the satellites  $A_1, A_2$  and  $C_1, C_2$  correspond to  $A_0$  and  $C_0$ , respectively. The correspondence between  $C_0$  and  $C_1, C_2$  is further supported by the fact that only these lines are associated with small spin-lattice relaxation rates ( $1/T_1$ ), so that their signals almost disappear at 10-msec rf-pulse repetition times. Since  $\nu_a + \nu_b + \nu_c = 0$ , the values of  $\nu_a$  are separately determined, although  $\nu_a$  and  $\nu_b$  cannot be distinguished from one another.

The site assignment for each set of resonance lines was made as follows. The satellite lines corresponding to the central line  $B_0$  show splittings  $B_i$  and  $B'_i$  ( $i=1-4$ ), which are associated with two distinct sites with slightly different values of  $\nu_c$  and almost equal values of  $K_c$ . These lines are assigned to the O(2) and O(3) sites, because these sites have very similar local environments and no other pairs could have such similarities. The axes of the largest EFG is either  $\hat{a}$  or  $\hat{b}$  for the lines  $A_0-A_2$  and  $\hat{c}$  for the lines  $C_0-C_2$ . The satellites  $A_0-A_2$  and  $C_0-C_2$  are therefore assigned to the O(1) and O(4) sites, respectively, because the direction of the largest EFG is very likely the Cu-O bond axis. The assignment of  $C_0-C_2$  to O(4) is also supported by the axial symmetry around the  $\hat{c}$  axis of the spin part of the shift  $K$  (see below). Our results on the O(2,3) and O(4) sites are consistent with those reported by Coretsopoulos *et al.*<sup>8</sup> Bleier *et al.* reported a narrow line with 0.024% shift and attributed it to the O(1) site.<sup>9</sup> We also observed a similar line but think it is a spurious signal, possibly from a second phase, because (1) we could not find any corresponding satellites and (2) the other lines already exhaust all the oxygen sites. There is no doubt that all of these lines arise from the correct phase because both the shift and  $1/T_1$  show a clear anomaly at the superconducting transition temperature, details of which will be described in separate papers.

Figure 2 shows the central (a) and the satellite (b) spectra with the field applied perpendicular to the  $c$  axis. These spectra show two-dimensional powder patterns because  $H_{\text{res}}$  is a function of field direction in the  $a$ - $b$  plane. The peaks in the satellite spectra are expected to occur when the field is along the  $\hat{a}$  or  $\hat{b}$  direction. Using the values of  $\nu_a$  and  $\nu_b$  determined from the Hllc spectra, the peaks are assigned as shown in Fig. 2(b)

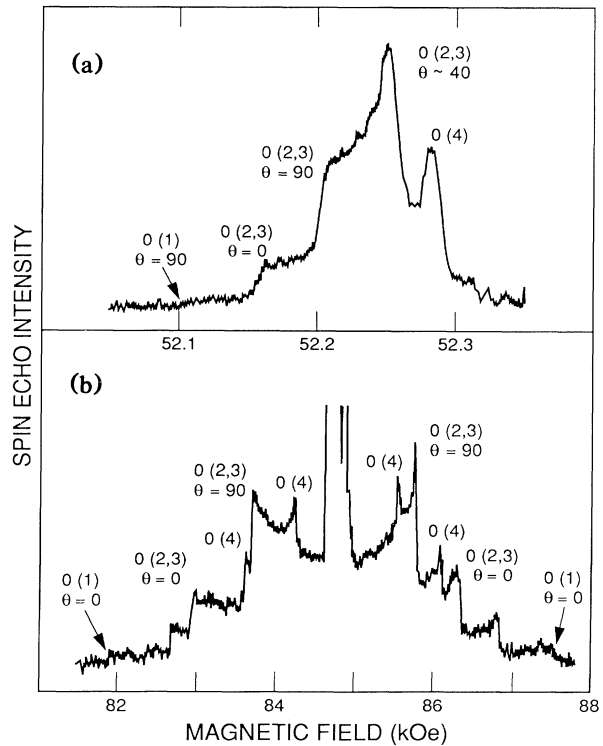


FIG. 2.  $^{17}\text{O}$  NMR spectra at 160 K with magnetic field perpendicular to the  $c$  axis. (a) The central transitions at 30.2 MHz and (b) the satellite transitions at 49.0 MHz.

(denotes field direction measured from the largest EFG axis). Values of  $K_a, K_b$  and refined values of  $\nu_a, \nu_b$  are obtained from Eq. (1b). The shift at O(1) for  $\theta=90^\circ$  was determined from the central-line spectrum using Eq. (1a) because the corresponding peaks in the satellite spectra are not clearly identified. All components of the derived EFG and  $K$  tensors are listed in Table I. The asymmetry factors ( $\eta$ ) of the EFG are 0.41 [O(1)], 0.22-0.23 [O(2,3)], and 0.32 [O(4)]. It should be noted that the values of  $\nu_a$  and  $K_a$  ( $a \perp c$ ) in the same row of Table I correspond to the same crystalline axis; we are not able, however, to associate these anisotropies with either the  $\hat{a}$  or  $\hat{b}$  crystal axis.

We first consider the results for the EFG. The frequencies  $\nu_a$  ( $a=a, b, c$ ) can be expressed as the sum of two terms<sup>10</sup>

$$\nu_a = (1 - \gamma) \nu_{a,l} + \nu_{a,h}. \quad (2)$$

Here  $\nu_{a,l}$  is the contribution from charges on the lattice ions, and  $\nu_{a,h}$  is the contribution from the on-site holes. The ionic charges distort the on-site electronic charge distribution and this effect is accounted for by the Sternheimer factor  $\gamma$ . The assignment of a  $\text{Cu}^{2+}$  valence is consistent with core-level x-ray-photoemission spectroscopy,<sup>11</sup> the EFG at both Cu sites,<sup>12,13</sup> and the anisotropy of the Cu Knight shifts and  $1/T_1$ .<sup>12,14</sup> We then assume the ionic charges  $\text{Y}^{3+}$ ,  $\text{Ba}^{2+}$ ,  $\text{Cu}^{2+}$ , and

TABLE I. EFG and  $K$  tensors. Two values of  $v_a$  in the parenthesis correspond to the O(2) and O(3) sites. Typical errors in  $v_a$  and  $K_a$  at 160 K are  $\pm 0.005$  MHz and 0.005%. Large errors in the values of  $K_a$  at 30 K are due to the uncertainty in the magnetic field inside the superconductor in the mixed state. This is estimated as described in Ref. 14.

	$v_a$ (MHz)	$K_a$ (%)		$K_s$ (%)
		160 K	30 K	
O(1)				
$\perp c$	-0.484	0.23	...	...
	(1.629)	0.22	$0.13 \pm 0.01$	$0.09 \pm 0.01$
$\parallel c$	-1.145	0.24	$0.13 \pm 0.03$	$0.11 \pm 0.03$
O(2,3)				
$\perp c$	(0.986)	0.31	$0.05 \pm 0.01$	$0.26 \pm 0.01$
	(0.966)			
	-0.598	0.17	$0.01 \pm 0.01$	$0.16 \pm 0.01$
$\parallel c$	(-0.387)	0.18	$0.02 \pm 0.03$	$0.16 \pm 0.03$
	(-0.369)			
O(4)				
$\perp c$	-0.375	-0.02	$-0.01 \pm 0.01$	$-0.01 \pm 0.01$
	-0.721	0.03	$0.04 \pm 0.01$	$-0.01 \pm 0.01$
$\parallel c$	1.096	0.08	$0.03 \pm 0.03$	$0.05 \pm 0.03$

$O^{13/7-}$ , which is consistent with one hole per unit cell. Using a point-charge model,  $(v_a, v_b, v_c)_i$  are calculated in units of MHz as

$$\begin{aligned}
 \text{O(1): } & (-0.0209, 0.0798, -0.0589), \quad \eta = 0.48, \\
 \text{O(2): } & (0.0631, -0.0245, -0.0386), \quad \eta = 0.22, \\
 \text{O(3): } & (-0.0208, 0.0539, -0.0331), \quad \eta = 0.23, \\
 \text{O(4): } & (-0.0160, -0.0455, 0.0615), \quad \eta = 0.48.
 \end{aligned} \tag{3}$$

For each site, the values of  $v_{a,i}$  are positive and largest along the Cu-O bond axis, and the asymmetries are modest ( $\eta < 0.5$ ). The value of  $\gamma$  is not known but should be larger than that for  $\text{Na}^+$  ( $\gamma = 4.6$ ) because  $\text{O}^{2-}$  has a larger ionic radius.<sup>10</sup> We now discuss the second contribution  $v_{a,h}$ . A single hole in the  $p_i$  orbital ( $i = x, y, z$ ) produces an axial EFG whose largest component is along the  $i$  direction and is given by  $v_{i,h} = (\frac{3}{20})(\frac{4}{5})e^2|Q| \times \langle r^{-3} \rangle$ . Setting  $\langle r^{-3} \rangle = 3.63$  a.u., which is 70% of the free-atom value,<sup>15</sup> we calculate for  $i = a$   $v_{a,h} = (2.66, -1.33, -1.33)h$ , where  $h$  is the fractional hole occupancy in the  $p_i$  orbital. It is possible that the holes occupy more than one  $p$  orbital, but this requires an accidental degeneracy which is less probable. It is therefore simplest to assume that  $h = \frac{1}{7}$  at each site. We consider two possible directions for the largest EFG at the O(2,3) sites: parallel (case I) and perpendicular (case II) to the bond axis. For case I, we find reasonable agreement between Eq. (2) and the measured values by taking  $\gamma = -9$ ,  $h = \frac{1}{7}$ , and  $i$  parallel to the bond axis:  $v_a(\text{meas}) = (0.976, -0.598, -0.378)$  and  $v_a(\text{calc}) = (0.97, -0.42,$

$-0.55)$ . [Here we have taken the average measured EFG for O(2) and O(3). The first number denotes the component along the bond axis.] For case II, on the other hand, values of  $v_a(\text{meas}) = \pm(-0.598, 0.976, -0.378)$  are not consistent with any reasonable choice of  $\gamma$  ( $\gtrsim 5$ ) and  $h$  (0-0.25). [For example, the values of  $\gamma = -9$  and  $h = \frac{1}{7}$  give  $v_a(\text{calc}) = (0.40, 0.15, -0.55)$  when  $i$  is perpendicular to the bond axis.] We therefore conclude that the direction of largest EFG at the O(2,3) sites is most likely along the Cu-O bond axis.

We next consider the shift results. Both the spin and the orbital magnetic moments could contribute to  $K$ ,  $K = K_s + K_{\text{orb}}$ .  $K_s$  is expected to be small at low temperatures in the superconducting state, while  $K_{\text{orb}}$  will be temperature independent, as discussed in the analysis of Cu Knight shift.<sup>14</sup>  $K_{\text{orb}}$  may therefore be approximated by the values of  $K$  at 30 K, which are also listed in Table I. We will focus on the anisotropic part of  $K_s$ , defined as  $K_{\text{ax}} = (K_s^{\parallel} - K_s^{\perp})/3$  for the uniaxial case, because this quantity is related to the spin density of the O  $p$  orbitals. (The isotropic part of  $K_s$  is mainly due to the contact field from the O  $2s$  orbital.<sup>16</sup>) The anisotropic hyperfine (dipolar) field from a singly occupied  $p_z$  state is  $2A_p \times (-\langle s_x \rangle, -\langle s_y \rangle, 2\langle s_z \rangle)$ , where  $A_p = \frac{2}{5} \mu_B \langle r^{-3} \rangle = 91 \text{ kOe}/\mu_B$ .<sup>16</sup> Note that this field is positive and larger along the direction of the lobes of the  $p$  orbital. At the O(2,3) sites,  $K_s$  is largest and shows uniaxial anisotropy around the axis of the largest EFG, i.e., the bond axis. The O(4) sites show an anisotropy of  $K$  in the  $a$ - $b$  plane, which is mostly of orbital origin. The spin part  $K_s$  for O(4) is nearly uniaxial and largest along the  $c$  axis. These facts give direct evidence that the spin density on the O(2,3) and O(4) sites resides mostly on the  $p_{\sigma}$  orbitals with lobes pointing along the bond axis. We note, however, that the anisotropy of  $K_{\text{orb}}$  (largest along the bond axis) for O(2,3) is not simply explained by unfilled  $p_{\sigma}$  orbitals, a fact which we do not understand. The anisotropy of  $K_s$  is small at the O(1) sites, meaning that either that the  $2p$  states do not carry appreciable spin density or that both  $p_{\sigma}$  and  $p_{\pi}$  states contribute to  $K_s$ , thereby reducing the anisotropy. It is rather surprising that the O(1) and O(4) sites show quite different magnitudes and anisotropies of  $K_s$  and  $K_{\text{orb}}$ .

The measured anisotropy of  $K_s$  can be used to estimate the spin susceptibility from the O  $p_{\sigma}$  states so that the total spin susceptibility can be decomposed into Cu  $d$  ( $\chi_d$ ) and O  $p$  ( $\chi_p$ ) parts. We ignore the contribution from the O(1) sites since the number of O(1) sites is only  $\frac{1}{7}$  of the total oxygen sites and assume equal spin susceptibility for both Cu sites. Thus

$$\chi_s = 3\chi_d + 4\chi_{p,\text{pl}} + 2\chi_{p,\text{br}}, \tag{4}$$

where  $\chi_{p,\text{pl}}$  ( $\chi_{p,\text{br}}$ ) is the contribution from the O(2,3) [O(4)] sites.  $K_{\text{ax}}$  at the O(2,3) sites is

$$K_{\text{ax,pl}} = (\chi_d A_{d,\text{pl}} + \chi_{p,\text{pl}} A_p) / N_A \mu_B. \tag{5}$$

Here  $A_{d,pl}$  is the dipole field from neighboring Cu sites. A similar expression holds for the O(4) sites. Using the values  $\chi_s = 3.23 \times 10^{-4}$  emu/mole,  $K_{ax,pl} = 3.3 \times 10^{-4}$ ,  $K_{ax,br} = 2.0 \times 10^{-4}$ ,  $A_{d,pl} = 2.3$  kOe, and  $A_{d,br} = 2.1$  kOe, we obtain  $\chi_d = 7.5$ ,  $\chi_{p,pl} = 1.8$ ,  $\chi_{p,br} = 1.1$  ( $\times 10^{-5}$  emu/mole). The entire O  $p$  contribution  $\chi_p = 4\chi_{p,pl} + 2\chi_{p,br} = 9.4 \times 10^{-5}$  emu/mole is 300% of the total  $\chi_s$ . Therefore, the dominant contribution to the spin susceptibility comes from Cu  $d$  states.

It is important to know how much of this spin density is associated with the doped-hole carriers, because even in the undoped system (YBa<sub>2</sub>Cu<sub>3</sub>O<sub>6.0</sub>) covalency produces a finite spin density on the O  $p_\sigma$  orbitals. This is transferred from the Cu  $d_{x^2-y^2}$  states, as has been observed in typical magnetic insulators.<sup>16</sup> This transferred spin density is so strongly coupled to the Cu  $d$  spin that both are treated as parts of a single spin system.

$\chi_p/\chi_s$  for the undoped system may be estimated from the calculation of Mila and Rice<sup>17</sup> who explicitly calculate the hybridized molecular orbitals. One obtains  $\chi_p/\chi_s = 0.10$  ( $\chi_{p,pl}/\chi_s = 0.019$ ,  $\chi_{p,br}/\chi_s = 0.013$ ) which is considerably smaller than the value obtained above for the fully oxygenated material ( $\chi_p/\chi_s = 0.3$ ). This difference may be interpreted as the contribution from the additional holes doped into the  $p_\sigma$  orbitals. In this case, the doped material would be described in terms of two separate, but coupled spin systems. On the other hand, because of the large uncertainty in the estimation of the transferred spin density and in light of the huge superexchange [ $J \sim 0.1$  eV (Ref. 18)] in the undoped system,  $\chi_p/\chi_s$  in the undoped system could be almost as large as that in the fully oxygenated material. In this case, the spin susceptibility of the doped holes must be very small compared with that of Cu  $d$  spins. This case would support the model that doped-hole spins make local singlet states with neighboring Cu  $d$  spins.<sup>19</sup> It should be noted that in either case (formation of the local singlet states or two spin systems) the doped holes reside in the  $p_\sigma$  orbitals. A clear distinction between these two cases should be made by experiments on the undoped system.

In conclusion, we present a complete identification of the NMR lines corresponding to all oxygen sites in YBa<sub>2</sub>Cu<sub>3</sub>O<sub>7</sub>. Measurements of the EFG and shift tensors clarify the different character of the various O sites. At the O(2,3) and O(4) sites, the spin density in the  $p_\sigma$  orbitals is likely to be responsible for the anisotropic

shift, taking the axis of the largest EFG along the Cu-O bond axis. This then requires that doped holes go into these  $p_\sigma$  orbitals, independent of whether the oxygen holes form local singlets with the Cu spins or have distinct degrees of freedom. For both cases, we expect a strong hybridization between doped-hole states and Cu  $d$ -spin states in the CuO<sub>2</sub> planes, resulting in a strong antiferromagnetic coupling between them.<sup>19,20</sup> This seems to be consistent with the observed rapid decrease in the Cu Knight shifts<sup>14</sup> and Cu(2) nuclear relaxation rates<sup>21</sup> below  $T_c$ , which clearly shows that Cu  $d$  spins are involved in the pairing.

We appreciate stimulating discussion with D. Pines, S. Trugman, F. J. Adrian, R. E. Walstedt, and W. W. Warren. We thank E. J. Peterson for technical assistance. This work was performed under the auspices of the U.S. Department of Energy.

- 
- <sup>1</sup>A. Fujimori *et al.*, Phys. Rev. B **35**, 8814 (1987).  
<sup>2</sup>N. Nucker *et al.*, Phys. Rev. B **37**, 5158 (1988).  
<sup>3</sup>A. Bianconi *et al.*, Phys. Rev. B **38**, 7196 (1988).  
<sup>4</sup>P. S. List *et al.* (unpublished).  
<sup>5</sup>V. J. Emery, Mat. Res. Bull. **14**, 67 (1989).  
<sup>6</sup>M. Takigawa *et al.*, Phys. Rev. B **39**, 300 (1989).  
<sup>7</sup>A. Abragam, *Principles of Nuclear Magnetism* (Clarendon, Oxford, 1961).  
<sup>8</sup>C. Coretsopoulos *et al.*, Phys. Rev. B **39**, 781 (1989).  
<sup>9</sup>H. Bleier *et al.*, J. Phys. (Paris) **49**, 1825 (1988).  
<sup>10</sup>M. H. Cohen and F. Reif, Solid State Phys. **5**, 321 (1957).  
<sup>11</sup>P. Steiner *et al.*, Z. Phys. B **69**, 449 (1988).  
<sup>12</sup>C. H. Pennington *et al.*, Phys. Rev. B **39**, 2902 (1989).  
<sup>13</sup>F. Adrian, Phys. Rev. B **38**, 2426 (1988).  
<sup>14</sup>M. Takigawa *et al.*, Phys. Rev. B **39**, 7371 (1989).  
<sup>15</sup>J. S. M. Harvey, Proc. Roy. Soc. London A **285**, 581 (1965).  
<sup>16</sup>A. Abragam and B. Bleaney, *Electron Paramagnetic Resonance of Transition Ions* (Clarendon, Oxford, 1970); J. Owen and J. H. M. Thornley, Rep. Prog. Phys. **29**, 675 (1966).  
<sup>17</sup>F. Mila and T. M. Rice, Physica (Amsterdam) **157C**, 561 (1989).  
<sup>18</sup>K. B. Lyons *et al.*, Phys. Rev. Lett. **60**, 732 (1988).  
<sup>19</sup>F. C. Zhang and T. M. Rice, Phys. Rev. B **37**, 3759 (1988).  
<sup>20</sup>V. J. Emery and G. Reiter, Phys. Rev. B **38**, 4547 (1988).  
<sup>21</sup>W. W. Warren, Jr., *et al.*, Phys. Rev. Lett. **59**, 11860 (1987).